J Mater Sci: Mater Med (2007) 18:119–125
DOI 10.1007/s10856-006-0669-6

# Fatigue limits and SEM/TEM observations of fracture characteristics for three Pd—Ag dental casting alloys

**Dongfa Li · William A. Brantley · Wenhua Guo · William A. T. Clark · Satish B. Alapati · Reza H. Heshmati · Glenn S. Daehn**

Received: 16 September 2005 / Accepted: 14 November 2005


**Abstract** The fatigue limits and fracture characteristics for three Pd–Ag dental casting alloys (Super Star, Heraeus Kulzer; Rx 91, Pentron; W-1, Ivoclar Vivadent) were studied. Specimens meeting the dimensions for ADA Specifications No. 5 and 38, and having the as-cast surface condition, were subjected to heat treatment simulating dental porcelain firing cycles and fatigued in air at room temperature under uniaxial tension-compression at 10 Hz. A ratio of compressive stress amplitude to tensile stress amplitude (R-ratio) of $-1$ was used. Alloy microstructures and fracture surfaces were examined with a scanning electron microscope and a transmission electron microscope. Fatigue limits for the three alloys had low values of approximately 15% of the yield strength for 0.2% permanent tensile strain. Complex fracture surfaces with characteristic striations were observed for all three fatigued alloys. Planar slip of dislocations occurred in the Pd solid solution matrix, along with dislocation-precipitate interactions and dislocation networks in the interfaces between the precipitates and surrounding matrix. Twinning occurred in the Pd solid solution matrix of Rx 91, and within discontinuous precipitates in Super Star and Rx 91. The low fatigue limits for these alloys are attributed to their complex microstructures and perhaps to casting defects.

D. Li · S. B. Alapati
PhD graduate student in Oral Biology, The Ohio State University, Columbus, OH, USA

W. A. Brantley · W. Guo · R. H. Heshmati
Section of Restorative and Prosthetic Dentistry, College of Dentistry, The Ohio State University, Columbus, OH, USA

W. A. T. Clark · G. S. Daehn
Department of Materials Science and Engineering, The Ohio State University, Columbus, OH, USA

W. Guo
Center for Biological and Environmental Nanotechnology (CBEN), Rice University, Houston, TX, USA

W. A. Brantley (✉)
Section of Restorative and Prosthetic Dentistry, College of Dentistry, The Ohio State University, PO Box 182357, Columbus, OH, USA 43218–2357
e-mail: brantley.1@osu.edu and wbrantle@columbus.rr.com

## 1 Introduction

Palladium–silver (Pd–Ag) dental casting alloys were introduced in the early 1970's as an economic alternative to gold casting alloys for metal-ceramic restorations [1–3] and have achieved widespread clinical popularity. These alloys are also used for the superstructures of dental implants. The Pd–Ag alloys usually contain between 50% and 60% Pd and 30% to 40% Ag (wt.%), with small amounts of low melting point metals, In and Sn, which promote strong bonding to dental porcelain and may improve castability by increasing molten metal fluidity. These alloys have a high elastic modulus which provides rigidity for multi-unit castings, high sag resistance during the porcelain firing cycles, excellent porcelain-metal bond strength, favorable handling and soldering characteristics, and satisfactory tarnish and corrosion resistance [1–13]. The Pd content is much lower in the Pd–Ag alloys than in the high-Pd dental alloys, and the former have become more attractive for clinical selection because of the recent Pd price volatility.

The main problem for clinical selection of Pd–Ag alloys has been their tendency to cause porcelain discoloration, which varies among different brands of dental porcelain. This problem has been alleviated or eliminated by proper melting and casting of these alloys, and selection of particular brands of porcelain [2, 3, 12, 14–16]. Other approaches

to prevent porcelain discoloration have included the use of coating agents and the incorporation of certain elements in the alloy composition [15, 17].

Fatigue is a fracture mode in which a metallic component fails after being subjected to repeated stresses that are substantially below its yield strength [18–20]. While there appears to be some clinical evidence that the failures of cast dental alloys *in vivo* can be related to cyclic fatigue rather than to an episode of acute overload [21], little published information is available on their fatigue properties. In previous studies, the fatigue limits and fracture characteristics for two high-Pd alloys, a Pd–Cu–Ga alloy and a Pd–Ga alloy not containing copper, were reported [22, 23]. The purpose of the present study was to investigate the fatigue behavior of three commercial Pd–Ag dental alloys; such information has not been previously reported.

## 2 Materials and methods

The Pd–Ag dental alloys selected for study were Super Star (Heraeus Kulzer, Armonk, NY, USA), Rx 91 (Pentron, Wallingford, CT, USA) and W-1 (Ivoclar Vivadent, Amherst, NY, USA). The nominal compositions and mechanical properties provided by the manufacturers are given in Tables 1 and 2.

Procedures for preparing the cast specimens, performing the fatigue experiments, and examining the fractured specimens with the scanning electron microscope (SEM) and transmission electron microscope (TEM) were the same as in recent studies [22, 23]. The alloys were melted using a gas-air torch and cast into tensile test bars having gauge diameter of 3 mm and gauge length of 15 mm [24, 25]. Polystyrene patterns (Salco, Romeoville, IL, USA) [26] conforming to these dimensions were invested in a carbon-free phosphate-bonded investment (Cera-Fina, Whip-Mix, Louisville, KY, USA). Two specimens of each alloy were cast for each fatigue stress amplitude and bench-cooled to room temperature, as recommended by the manufacturer. Sprues were cut from the cast specimens with a carborundum disk, and any visible nodules were removed.

Specimens in the as-cast surface condition, without subsequent air-abrasion or polishing, were subjected to heat treatment in a conventional dental porcelain furnace (Ultra-Mat CDF, 3 M Unitek, Monrovia, CA, USA) that simulated the porcelain-firing cycles. The initial oxidation step followed the instructions of each alloy manufacturer, and the subsequent firing cycles followed the recommendations for IPS Classic porcelain (Ivoclar Vivadent). For the W-1 alloy only, a special hardening heat treatment at 650°C indicated by the manufacturer was performed before the simulated heat treatment cycles for porcelain application.

Calculations of loads required to produce the desired stress amplitudes for fatigue testing were based on the values of yield strength (YS) for 0.2% permanent tensile strain ($\sigma_{0.2}$) provided by the manufacturers for the alloys in the heat-treated condition for porcelain bonding (Table 2): 655 MPa for Super Star, 660 MPa for Rx 91, and 605 MPa for W-1 (hardening heat treatment). Measurement of the 0.2% YS is stipulated in the specification for metal-ceramic systems [25], in which a minimum value of 250 MPa is required for a ceramic alloy.

Fatigue tests were carried out in air at room temperature using uniaxial sinusoidal tension-compression loading (Model 1322, Instron Corp., Canton, MA, USA). The ratio (R-ratio) between the compressive and tensile stress amplitudes was –1, and the frequency was 10 Hz. Selection of the starting stress amplitude was based on previous experience with dental high-Pd casting alloys [22], which resulted in considerably fewer specimens than with the conventional

**Table 1** Nominal compositions (wt %) of Super Star, Rx 91, and W-1 Pd—Ag dental alloys provided by manufacturers

| Alloy | Pd | Ag | Sn | In | Other |
|---|---|---|---|---|---|
| Super Star* | 59.8 | 28.1 | 5.0 | 6.0 | <1.0 Ga, Ru and Re |
| Rx 91† | 53.5 | 37.5 | 8.5 | <1.0 | <1.0 Ru |
| W-1‡ | 53.3 | 37.7 | 8.5 | <1.0 | <1.0 Ru and Li |

*Heraeus Kulzer, Armonk, NY, USA. [Website: www.heraeus-kulzer-us.com]
†Pentron, Wallingford, CT, USA. [Website:www.pentron.com]
‡Ivoclar Vivadent, Amherst, NY, USA. [Website: www.ivoclarvivadent.us.com]

**Table 2** Nominal mechanical properties for Super Star, Rx 91, and W-1 Pd—Ag dental alloys provided by manufacturers (after heat treatment for porcelain application)

| Alloy | Elastic modulus (GPa) | 0.2% Yield strength [$\sigma_{0.2}$] (MPa) | Percentage elongation (%) | Vickers hardness |
|---|---|---|---|---|
| Super Star | 130 | 655 | 15 | 285 |
| Rx 91 | 130 | 660 | 14 | 235 |
| W-1 | –¶ | 485 | 11 | 240 |
| | | 605 (hardening heat treatment) | | |

¶Not reported.

staircase method [19]. Two replicate specimens were tested at each stress amplitude, and the amplitude at which fracture did not occur after $2 \times 10^6$ cycles was designated as the fatigue limit. This number of cycles provided clinical relevance [21], without unduly prolonging the testing period.

After ultrasonic cleaning in ethanol, the surfaces of the fatigued specimens were examined with an SEM (JSM-820, JEOL Ltd, Tokyo, Japan) over a range of magnifications. Microstructural observations were carried out with the same SEM on flat samples sectioned from the fractured bars by a slow-speed water-cooled diamond saw, and mounted in transparent metallographic epoxy resin (Leco, St. Joseph, MI, USA). After grinding with 320, 400, and 600 grit silicon carbide papers and polishing with a series of $Al_2O_3$ slurries ending with 0.05 $\mu$m particles, specimens were etched in aqua regia solutions to reveal their microstructures.

Specimens that fractured during the fatigue test were also examined by TEM (Philips CM 200, Eindhoven, The Netherlands). Regions near the fracture surface were cut from the fatigued specimen using the same low-speed, water-cooled diamond saw. These slices were mechanically ground to a thickness of about 100 $\mu$m and punched to form approximately 3 mm diameter disks, which were dimpled using 1 $\mu$m and 0.5 $\mu$m diamond gels to a thickness of 30–40 $\mu$m. These resulting foils were further thinned to electron transparency using an argon ion miller, and their surfaces were plasma-cleaned to eliminate any preparation artifacts. The TEM observations were performed over a range of magnifications at an operating voltage of 200 keV.

## 3 Results

### 3.1 Microstructures and fatigue limits of Pd—Ag alloys

As-cast Rx 91 had an equiaxed fine-grain microstructure, while as-cast W-1 had a dendritic microstructure. As-cast Super Star had inhomogeneous, equiaxed, grain-like regions with a dendritic character that was previously reported [27]. These general microstructures were maintained after simulated porcelain-firing heat treatment, as shown in Fig. 1 (a), (b) and (c), and spherical precipitates were observed in the Pd solid solution matrix of all three alloys. Discontinuous precipitates also appeared in the grain boundaries of Super Star and Rx 91 and in the dendritic structure of W-1 after the heat treatment. Little porosity was observed in the three Pd–Ag alloys, which was similar to previous results for cast high-Pd dental alloys [22, 28, 29], although there were areas of each specimen with more substantial porosity. Table 3 shows the number of cycles for failure at different stress amplitudes and that the fatigue strength of Super Star, Rx 91 and W-1 for the heat-treated condition is approximately 15% of the 0.2% offset yield strength ($\sigma_{0.2}$).

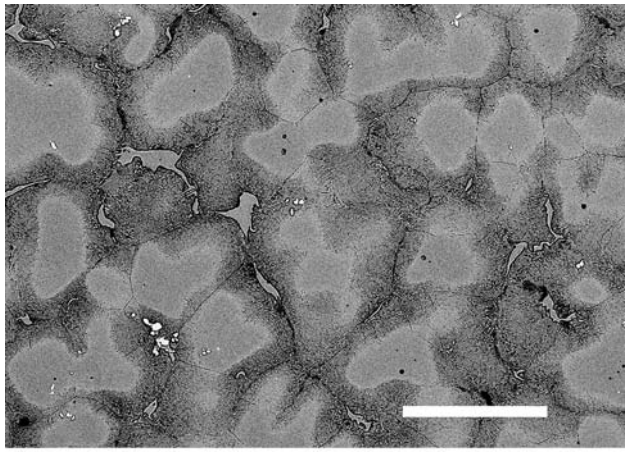

(a)

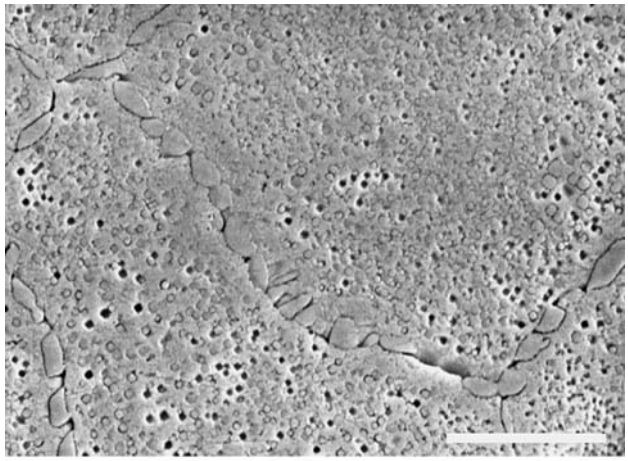

(b)

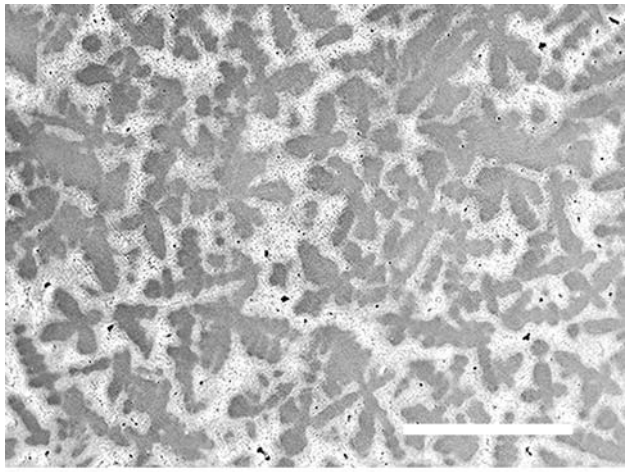

(c)

**Fig. 1** SEM images of heat-treated (a) Super Star (scale bar length = 50 $\mu$m), (b) Rx 91 (scale bar length = 4 $\mu$m), and (c) W-1 (scale bar length = 300 $\mu$m). Fig. 1 (a) is a backscattered electron image, and (b) and (c) are secondary electron images. The as-cast dendritic character of W-1 is maintained after the porcelain-firing heat treatment. The inhomogeneous compositions of the equiaxed regions with dendritic character in Super Star are evident in the backscattered electron image. The higher-magnification photomicrograph of Rx 91 shows the discontinuous grain boundary precipitates and the etching pattern within grains.

**Table 3** Fatigue cycles to failure for Super Star, Rx 91, and W-1

| Specimen no. | Alloy | Stress* (Load, N) | Fatigue cycles |
|---|---|---|---|
| 1 | Super Star | $0.20\sigma_{0.2}$ (926) | 350,292 |
| 2 | | $0.20\sigma_{0.2}$ (926) | 715,875 |
| 3 | | $0.15\sigma_{0.2}$ (695) | 1,516,640 |
| 4 | | $0.15\sigma_{0.2}$ (695) | >2,000,000 |
| 5 | Rx 91 | $0.15\sigma_{0.2}$ (700) | 983,905 |
| 6 | | $0.15\sigma_{0.2}$ (700) | 1,226,010 |
| 7 | | $0.10\sigma_{0.2}$ (467) | >2,000,000 |
| 8 | | $0.10\sigma_{0.2}$ (467) | >2,000,000 |
| 9 | W-1† | $0.20\sigma_{0.2}$ (855) | 907,330 |
| 10 | | $0.20\sigma_{0.2}$ (855) | 183,210 |
| 11 | | $0.15\sigma_{0.2}$ (642) | 659,555 |
| 12 | | $0.15\sigma_{0.2}$ (642) | >2,000,000 |

*Values of stress have been rounded to the nearest $0.05\sigma_{0.2}$.
†Values of stress are based upon a value of 605 MPa for $\sigma_{0.2}$ (Table 2).

## 3.2 Fracture and microstructural characteristics of fatigued Pd—Ag alloys

### *3.2.1 SEM characterization of the fatigue fracture surface*

SEM observations showed that the fatigue crack responsible for failure initiated either at the surface or inside the specimens, although it was usually impossible to determine unambiguously the actual site of initiation. Figure 2 shows an apparent dendritic structure, within which incomplete solidification resulted in an absence of interdendritic regions, around the crack initiation region on the surface of one fatigued Super Star specimen.

Fine-scale fatigue striations similar to those for high-Pd dental alloys [22] were observed on the fracture surfaces of all three Pd–Ag alloys, as shown in Fig. 3 (a), (b) and (c), and many secondary cracks were also observed along these striations. For Super Star, some variation in the orientation of these striations was observed, as shown in Fig. 3 (a). Terraced patterns of striations were observed for all three Pd–Ag alloys, with the striations superimposed on coarser features; these features and the fatigue striations were approximately perpendicular to each other, as shown in Fig. 4 (a) and (b).

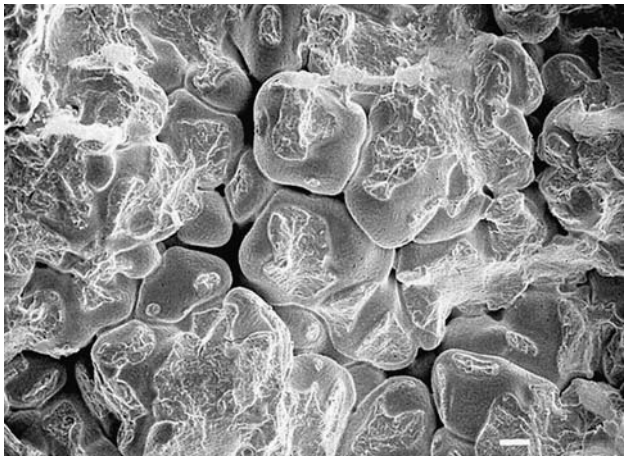

**Fig. 2** Secondary electron SEM image showing the incomplete solidification (dendritic structure) around the fatigue crack initiation region on the fracture surface of one Super Star alloy specimen, which failed after 1,516,640 cycles at $0.15\sigma_{0.2}$. (Scale bar length = 10 $\mu$m).

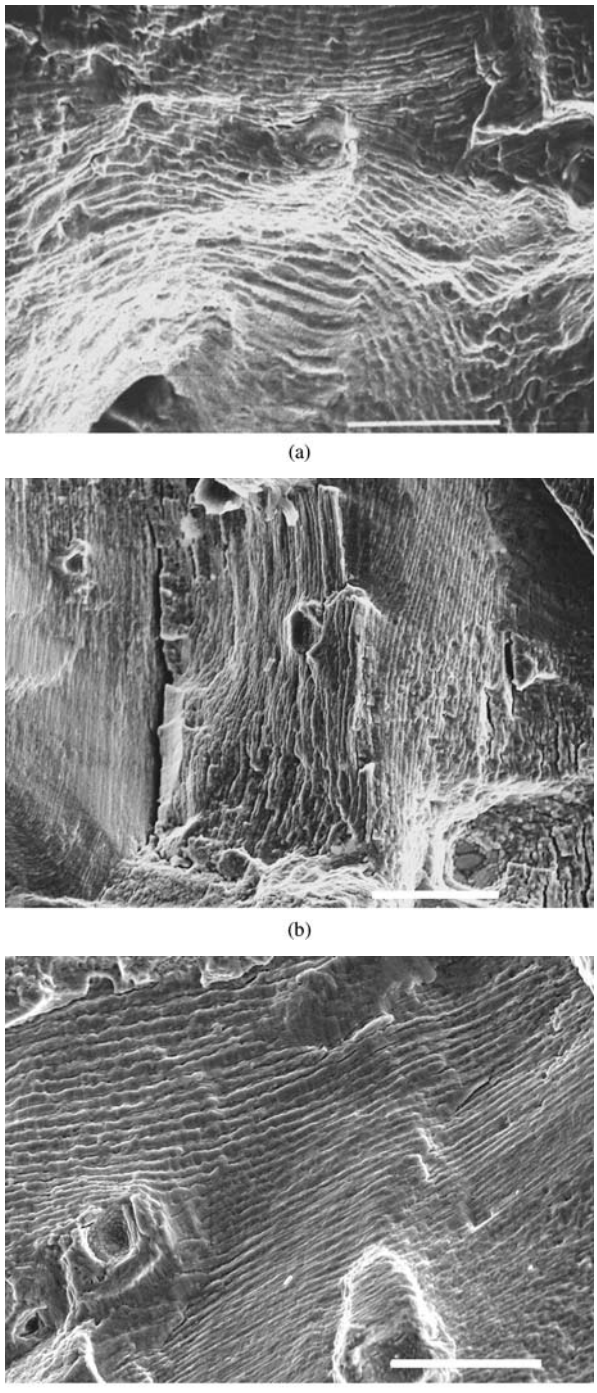


**Fig. 3** Secondary electron SEM images of fatigue fracture surfaces for (a) Super Star, 1,516,640 cycles at $0.15\sigma_{0.2}$ (scale bar length = 20 $\mu$m), (b) Rx 91, 1,226,010 cycles at $0.15\sigma_{0.2}$ (scale bar length = 10 $\mu$m), and (c) W-1, 907,330 cycles at $0.20\sigma_{0.2}$ (scale bar length = 10 $\mu$m), showing typical fatigue striations in the alloys.

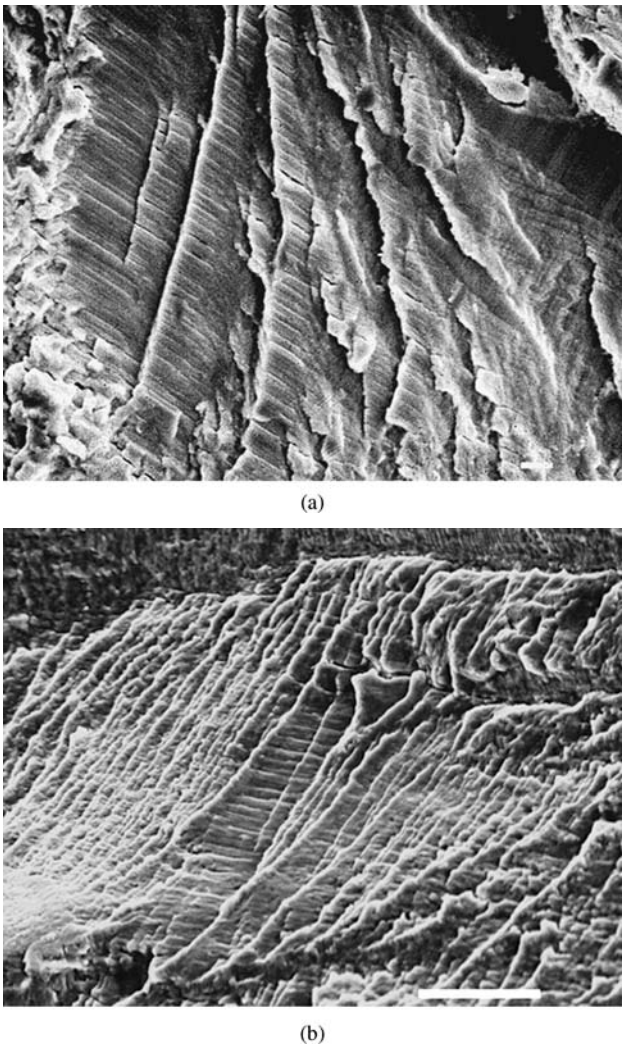

**Fig. 4** Secondary electron SEM images of the fatigue fracture surfaces for (a) Super Star, 715,875 cycles at $0.20\sigma_{0.2}$ (scale bar length = 1 $\mu$m) and (b) W-1, 659,555 cycles at $0.15\sigma_{0.2}$ (scale bar length = 5 $\mu$m), showing terraced patterns of striations.

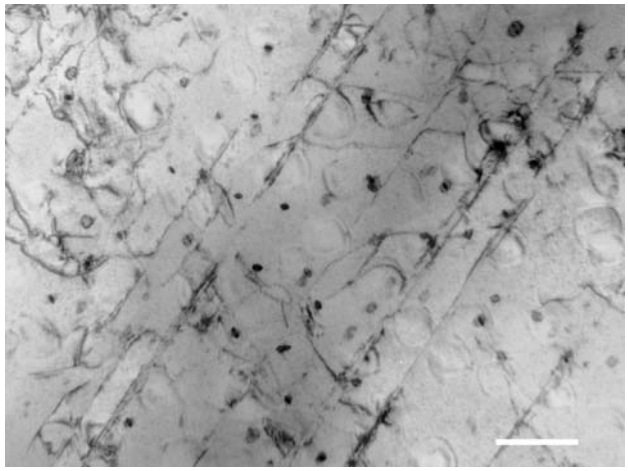

**Fig. 5** TEM bright-field image of tangled dislocations and stress-induced slip bands in fatigued W-1, 183,210 cycles at $0.20\sigma_{0.2}$. (Scale bar length = 200 nm.)

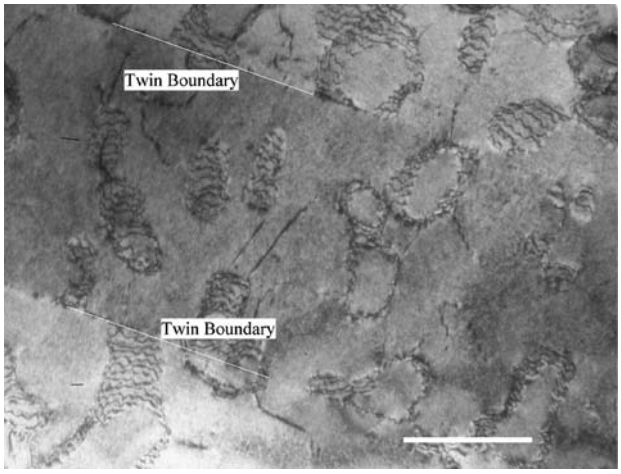


**Fig. 6** TEM bright-field image showing interphase boundary dislocations between the spherical precipitates and the surrounding twinned matrix of fatigued Rx 91, 1,226,010 cycles at $0.15\sigma_{0.2}$. (Scale bar length = 200 nm.)

### *3.2.2 TEM characterization of fatigued Pd—Ag alloys*

TEM observation revealed networks of tangled dislocations and stress-induced slip bands in fatigued specimens of all three alloys (Fig. 5), indicating the role of dislocation motion in the cyclic deformation process. Interactions between dislocations and the spherical precipitates, and dislocation networks in the interfaces between the precipitates and the surrounding matrix, were also observed (Fig. 6) and attributed to the effect of cyclic deformation. Twinning was also observed in the palladium solid solution matrix of Rx 91 (Fig. 6), and in the discontinuous precipitates in Super Star and Rx 91 (Fig. 7).

## 4 Discussion

The fatigue limit, which provides quantitative information about resistance of an alloy to failure by cyclic loading, is dependent upon the composition, microstructure, and numerous testing variables. These include the nature of the cyclic loading (*e.g.*, axial as in the present investigation, bending, or torsion), the stress amplitude, R-ratio, specimen size and shape, and the designated number of loading cycles corresponding to use conditions [19, 20]. A fatigue limit is meaningful only when all of these testing variables are specified, and comparisons of fatigue limits for different alloys are usually applicable only when the data are acquired under the same testing conditions. At present there are no American National Standard/American Dental Association or ISO (International Office for Standardization) specifications or

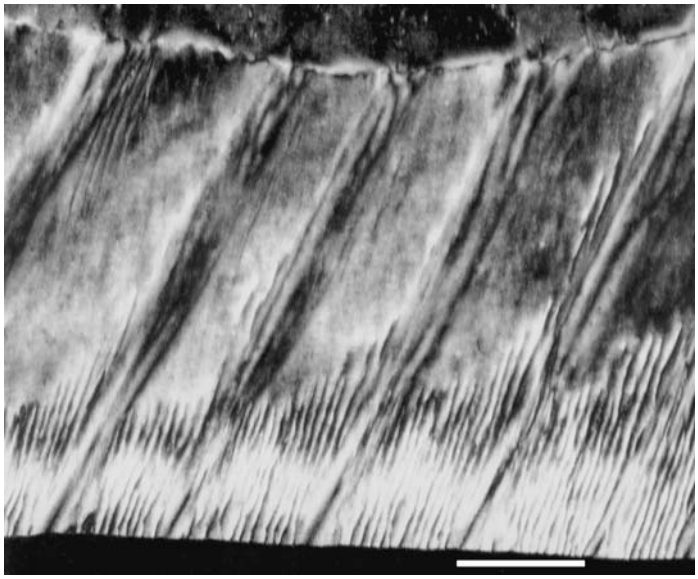

**Fig. 7** TEM dark-field image showing twinning inside discontinuous precipitates due to fatigue deformation in Rx 91, 983,905 cycles at $0.15\sigma_{0.2}$. (Scale bar length = 50 nm.)

widely accepted protocols for fatigue testing of dental casting alloys.

The fatigue limit to yield strength ($\sigma_{0.2}$) ratio for the three Pd–Ag alloys (Table 3) is similar to that for two high-Pd alloys tested under the same conditions [22]. In this previous study, the ratio of fatigue limit to yield strength of approximately 0.15–0.20 for two high-Pd alloys was calculated for the value of YS at 0.1% permanent tensile strain ($\sigma_{0.1}$). Recalculation of this ratio for the two high-Pd alloys using the $\sigma_{0.2}$value for yield strength only causes a minor change in the ratio of 0.15–0.20, which has little meaning given the accuracy of the experimental measurements involved. For example, the values of stress amplitude Table 3 have been rounded to the nearest $0.05\sigma_{0.2}$, which is consistent with the approximate $\sigma_{0.2}$ values reported by the manufacturers to the nearest 5 MPa (Table 2). Table 3 shows that there is a steep dependence of the number of fatigue cycles to failure on the stress amplitude ($\sigma_{0.2}$), and the results for Rx 91 suggest that its fatigue limit may be closer to $0.15\sigma_{0.2}$ than $0.10\sigma_{0.2}$. Consequently, the fatigue limit for the three Pd–Ag alloys is approximately $0.15\sigma_{0.2}$ for cast test specimens of the dimensions used in this study.

In a previous study on fatigue of high-Pd alloys [22], it was noted that the low ratio of fatigue limit to yield strength might be attributed to casting or microstructural defects in the cast specimens. Since casting defects cannot be completely eliminated from practical casting processes [30, 31], characterization of these defects (bulk porosity and surface flaws) and in the fatigue test specimens and their effects on fatigue properties are important areas for further investigation. In addition, the fatigue performances of castings with dimensions closer to those of single-tooth metal-ceramic restorations need to be determined. For such smaller test specimens and for the metal components of single-tooth metal-ceramic restorations, the results in Table 3 should be considered as conservative, lower-limit values of the fatigue limit for these alloys.

After the simulated porcelain-firing heat treatment, values of the nominal yield strength ($\sigma_{0.2}$) for Super Star, Rx 91 and W-1 are similar, using the value for W-1 after the hardening heat treatment (Table 2), and values for percentage elongation and Vickers hardness for these three Pd–Ag alloys are also similar. Small differences in these mechanical properties arise from differences in the alloy compositions (Table 1) and microstructures. For example, the lower percentage elongation for W-1, compared to Super Star and Rx 91, might be associated with differences in the dendritic structures of the three alloys, which would result in differences in the general paths for crack propagation through the interdendritic regions. In a previous study, a high-Pd alloy with a dendritic as-cast microstructure (Spartan Plus, Ivoclar Vivadent) had considerably greater percentage elongation after heat treatment simulating the porcelain firing cycles, which eliminated the as-cast dendritic microstructure [29].

The results in Table 3 thus suggest that under the conditions of the present study the fatigue limit is not greatly affected by whether the alloy has a dendritic or equiaxed fine-grained microstructure, or a combination of both types of microstructural constituents. The major factor for the maximum load at which fatigue failure does not occur for the Pd–Ag alloys (Table 3) is the yield strength, which is dependent upon the strengthening mechanisms for these alloys. Studies of these mechanisms will be reported in separate manuscripts that describe TEM observations of the annealed alloys.

Since dislocations tangles and stress-induced slip bands were observed by TEM in all three fatigued alloys (Fig. 5), slip was a common mode of permanent deformation. In addition, twinning was observed in the Pd solid solution matrix

of fatigued Rx 91 (Fig. 6), and in the discontinuous precipitates (Fig. 7) in fatigued Super Star and Rx 91, indicating that twinning was an additional mode of permanent deformation for these alloys. In previous studies [22, 23], the Pd–Cu–Ga alloy in which twinning was the main permanent deformation mode had superior fatigue resistance to the Pd–Ga alloy where such twinning was not observed. Therefore, the occurrence of twinning to relieve local stress concentrations during fatigue deformation may be beneficial to fatigue performance.

## 5 Conclusions

The fatigue limits of three Pd–Ag alloys, Super Star, Rx 91 and W-1, were investigated using uniaxial tension-compression loading with a stress amplitude ratio of $R = -1$. The microstructural and fracture characteristics of the fatigued specimens were analyzed by SEM and TEM. The following conclusions can be drawn from this study:

1. The fatigue limit (for $2 \times 10^6$ cycles) of the Super Star, Rx 91 and W-1 alloys was approximately 15% of the 0.2% offset yield strength in tension. The specimens had the original as-cast surface condition and were heat-treated to simulate the clinical firing cycles for dental porcelain.
2. The fatigue properties of the W-1 and Super Star alloys were not adversely affected by their dendritic microstructures, which had distinctly different character in the two alloys, that existed after the simulated porcelain-firing heat treatment.
3. During fatigue, slip in the Pd solid solution matrix is a common permanent deformation mechanism for all the three Pd–Ag alloys. Twinning provides an additional permanent deformation mode for Super Star and Rx 91.

**Acknowledgments** This study was supported by Grant DE 10147 from the National Institute of Dental and Craniofacial Research of the National Institute of Health, Bethesda, MD, USA. We would like to thank Lloyd Barnhart in the Department of Materials Science and Engineering for his expert technical assistance in the fatigue testing. We also thank Tridib Dasgupta, Director of Materials Research at Ivoclar Vivadent (US) for helpful comments on the properties of Pd–Ag alloys.

## References

1. E. F. HUGET and S. CIVJAN, *J. Am. Dent. Assoc.* **89** (1974) 383.
2. R. L. BERTOLOTTI, *J. Am. Dent. Assoc.* **108** (1984) 959.
3. C. J. GOODACRE, *J. Prosthet. Dent.* **62** (1989) 34.
4. E. F. HUGET, N. DVIVEDI and H. E. COSNER, *J. Prosthet. Dent.* **36** (1976) 58.
5. G. W. MYERS AND D. W. CRUICKSHANKS-BOYD, *Br. Dent. J.* **153** (1982) 323.
6. R. W. HINMAN, J. A. TESK, R. P. WHITLOCK, E. E. PARRY and J. S. DURKOWSKI, *J. Dent. Res.* **64** (1985) 134.
7. P. R. MEZGER, M. M. A. VRIJHOEF and E. H. GREENER, *J. Dent. Res.* **65** (1986) 748.
8. D. C. REEL, J. T. KEMPER, W. B. JONES and R. J. MITCHELL, *J. Dent. Res.* **64** (1986) 317 [abstract].
9. P. R. MEZGER, A. L. H. STOLS, M. M. A. VRIJHOEF and E. H. GREENER, *Dent. Mater.* **5** (1989) 350.
10. P. R. MEZGER, M. M. A. VRIJHOEF and E. H. GREENER, *Dent. Mater.* **5** (1989) 97.
11. E. PAPAZOGLOU and W. A. BRANTLEY, *Dent. Mater.* **14** (1998) 112.
12. W. A. BRANTLEY and L. W. LAUB, in "Contemporary Fixed Prosthodontics," 3rd edn., edited by S. F. Rosenstiel, M. F. Land and J. Fujimoto (Mosby, St. Louis, 2001), p. 497.
13. M. R. PINASCO, E. ANGELINI, E. CORDANO, E. MAGI and F. ROSALBINO, *J. Mater. Sci.: Mater. Med.* **11** (2000) 837.
14. A. M. LACY, R. HIROSE and M. D. JENDRESEN *J. Calif. Dent. Assoc.* **5** (1977) 44.
15. R. L. BERTOLOTTI, in "Proceedings of the Fourth International Symposium on Ceramics," edited by J. D. Preston, (Quintessence, Chicago, 1988), p. 79.
16. W. J. O'BRIEN, K. M. BOENKE, J. B. LINGER and C. L. GROH, *Dent. Mater.* **14** (1998) 365.
17. R. D. RINGLE, J. R. MACKERT and C. W. FAIRHURST, *J. Dent. Res.* **65** (1986) 218 [abstract].
18. M. C. NUTT, in "Metallurgy and Plastics for Engineers" (Pergamon Press, Oxford, 1976), p. 360.
19. G. E. DIETER, in "Mechanical Metallurgy" 3rd edn. (McGraw-Hill, New York, 1986), p. 329, 375.
20. N. E. DOWLING, in "Mechanical Behavior of Materials: Engineering Methods for Deformation, Fracture and Fatigue" (Prentice Hall, Englewood Cliffs, NJ, 1993). p. 339, 397 and 456.
21. H. W. ANSELM WISKOTT, J. I. NICHOLLS and U. C. BELSER, *Int. J. Prosthodont.* **8** (1995) 105.
22. D. LI, W. A. BRANTLEY, J. C. MITCHELL, G. S. DAEHN, P. MONAGHAN and E. PAPAZOGLOU, *J. Mater. Sci.: Mater. Med.* **13** (2002) 361.
23. W. H. GUO, W. A. BRANTLEY, D. LI, P. MONAGHAN and W. A. T. CLARK, *J. Mater. Sci.: Mater. Med.* **13** (2002) 369.
24. American National Standard/American Dental Association Specification No. 5 for dental casting alloys (American Dental Association, Council on Scientific Affairs, Chicago, 1997).
25. American National Standard/American Dental Association Specification No. 38 for metal-ceramic dental restorative systems (American Dental Association, Council on Scientific Affairs, Chicago, 2000).
26. D. A. BRIDGEPORT, W. A. BRANTLEY and P. F. HERMAN, *J. Prosthod.* **2** (1993) 144.
27. S. G. VERMILYEA, Z. CAI, W. A. BRANTLEY and J. C. MITCHELL, *J. Prosthodont.* **5** (1996) 288.
28. E. PAPAZOGLOU, Q. WU, W. A. BRANTLEY, J. C. MITCHELL and G. MEYRICK. *Cells Mater.* **9** (1999) 43.
29. E. PAPAZOGLOU, Q. WU, W. A. BRANTLEY, J. C. MITCHELL and G. MEYRICK. *J. Mater. Sci.: Mater. Med.* **11** (2000) 601.
30. K. J. ANUSAVICE, in "Phillips' Science of Dental Materials," 10th edn. (Saunders, Philadelphia, 1996), p. 517.
31. T. MIZUMOTO, M. NIINOMI, T. AKAHORI and H. FUHUI, *Mater. Sci. Forum* **426** Pt. 4 (2003) 3207.